Quantitative detection of DNA labeled with magnetic nanoparticles using arrays of MgO-based magnetic tunnel junction sensors

Weifeng Shen,[1,a)] Benaiah D. Schrag,[2] Matthew J. Carter,[2] and Gang Xiao[1,b)]
[1]*Physics Department, Brown University, Providence Rhode Island 02912, USA*
[2]*Micro Magnetics Inc., 421 Currant Road, Fall River, Massachusetts 02720, USA*

(Received 13 June 2008; accepted 27 June 2008; published online 22 July 2008)

We have demonstrated the detection of 2.5 μM target DNA labeled with 16 nm Fe_3O_4 nanoparticles (NPs) using arrays of magnetic tunnel junction sensors with (001)-oriented MgO barrier layers. A MTJ sensor bridge was designed to detect the presence of magnetic NPs bonded with target DNA. A raw signal of 72 μV was obtained using complementary target DNA, as compared with a nonspecific bonding signal of 25 μV from noncomplementary control DNA. Our results indicate that the current system's detection limit for analyte DNA is better than 100 nM. © *2008 American Institute of Physics*. [DOI: 10.1063/1.2963970]

In recent years, an intense effort has been made to design and develop biodetection systems which combine magnetic labels with magnetoresistance (MR) sensors, as a potential technological alternative to traditional devices using fluorescent markers.[1–3] The principle of these systems is to specifically attach magnetic labels to the analyte biomolecules, and then use the MR sensor(s) to detect the stray field generated by the embedded labels for biorecognition purposes.[4] The ultimate goal is to build a high-sensitivity, low-cost, and portable "all-in-one" biodetection system.[5] Compared to larger magnetic labels (sizes from 0.1 to 10 μm), magnetic nanoparticles (NPs) have a higher saturation magnetization and a better size match with the biomolecules to be detected, which makes them more attractive for high-sensitivity, quantitative biodetection applications.[6,7] Once suitably attached, such magnetic NPs can be also used to transport proteins, nucleic acids, and other biomolecules through microfluidic circuits, so that they may be bonded to the probe area of the biochip and detected by the MR sensors.

The giant MR (GMR) and tunneling TMR effects in thin film multilayers have been intensively studied as part of the emerging field of spintronics.[8] These technologies have also been widely employed in fully integrated magnetic bimolecular recognition assays.[9–11] Compared to GMR sensors, MgO-based magnetic tunnel junction (MTJ) sensors offer higher MR ratios and therefore higher magnetic field sensitivity.[12,13] As a result, MTJs are better suited for the accurate detection of the small magnetic fields (<1 Oe) which are typically encountered in most biomagnetic applications. In this paper, we report on the design and development of magnetic biosensors based on bridge structures composed of MTJ sensors with MgO tunnel barriers. We also demonstrate the use of these sensor bridges for the detection of 2.5 μM single-strand analyte DNA labeled with 16 nm diameter Fe_3O_4 NPs.

MTJ multilayer films were deposited on thermally oxidized Si wafers using a custom multitarget high-vacuum magnetron sputtering system (base pressure of 2×10^{-8} Torr). The MTJ stacks used in this study had the following layer structure: (thicknesses in nanometers): substrate/Ta (30)/$Co_{50}Fe_{50}$ (2)/IrMn (15)/$Co_{50}Fe_{50}$ (2)/Ru (0.8)/$Co_{40}Fe_{40}B_{20}$ (3)/MgO (1.4)/$Co_{40}Fe_{40}B_{20}$ (3)/Ta (10)/Ru (5). Micron-size (6×18 μm^2) elliptical junctions were patterned using standard optical lithography and ion milling. A 100-nm-thick gold layer was deposited on top of the junction area and patterned into low-resistance electrical contacts to the top of the MTJ junction. The detailed MTJ sensor fabrication processes which were employed are described in a previous work.[14] Typical MTJ sensors show MR ratio of 120% and a resistance-area (RA) product of 5 k Ω μm^2. Over the field range of ±10 Oe, a magnetic field sensitivity on the order of 1.0%/G is typical.

A patterned MTJ sensor bridge was designed to detect the presence of magnetic NPs bonded to the sensor area. The sensor bridge, shown in Fig. 1, contains 64 MTJ sensors in a Wheatstone bridge configuration, with 16 sensors in series comprising each arm. Each individual MTJ sensor has lateral dimensions of 6×18 μm. The biologically active area—indicated by the 120 μm diameter green circle in Fig. 1(a)—is spotted on top of the two sensing arms by a microspotter. We have chosen the size of this area to be identical to the standard spot size of commercial DNA microarray piezospotter devices. The two remaining arms in the bridge are used as references; these devices are covered with a SU-8 photoresist shield (5 μm in thickness) to prevent the bonding of any particles, as seen in Fig. 1(c). Figure 2(d) shows a close-up view of one 16-element arm of the bridge. Each sensor in the two sensing arms serves as a detection unit. When a layer of magnetic NPs is bonded onto the sensor surface, the bridge will generate a total signal proportional to the coverage of NPs, which is in turn related to the concentration of target molecules in the analyte sample.

The MTJ sensor bridge die was mounted on an open dual-inline socket with a flat surface so that microfluidic circuits could be integrated on top of the sensor surface. The whole chip was then plugged directly into a custom-made printed circuit board (PCB) designed for the prototyping experiments. The circuit board, into which the MTJ biosensor chip was plugged, was placed in the gap between two crossed pairs of toroidal electromagnets, which provide in-plane dc and ac magnetic fields. dc biasing fields are used to reduce the hysteresis of the MTJ biosensor, make the sensor response more linear and sensitive, and ensure that off-axis

a)Electronic mail: weifeng_shen@brown.edu.
b)Electronic mail: gang_xiao@brown.edu.

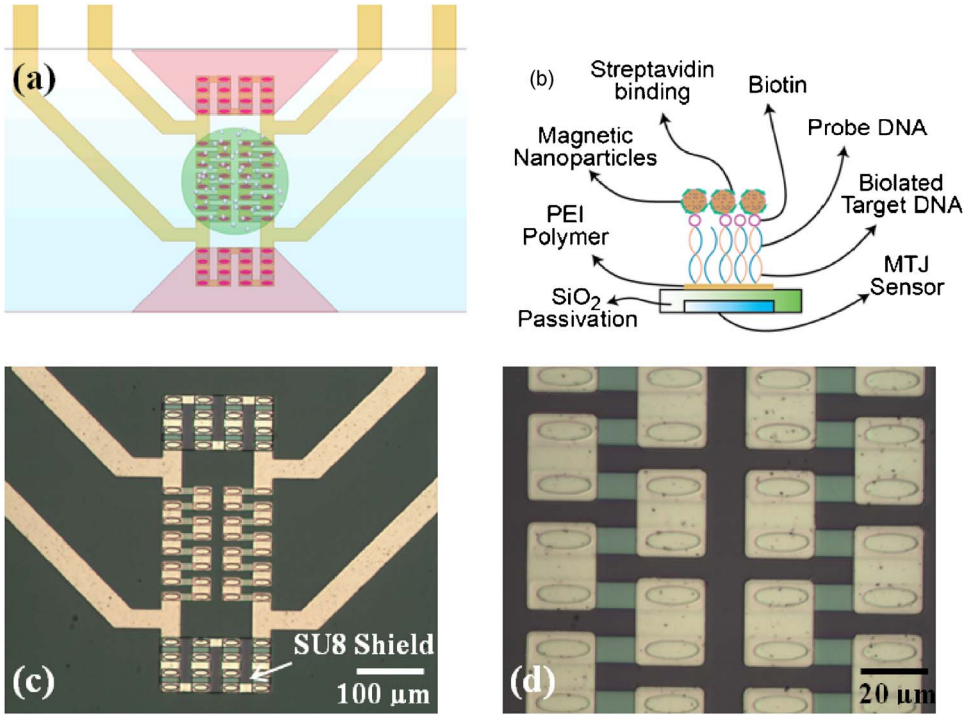

FIG. 1. (Color online) (a) Schematic image of the 64-element MTJ array. The 120 μm diameter green spot is the biologically active area which contains all of the active MTJ sensors. The pink area indicates the regions of photoresist which shield the reference arms of the Wheatstone bridge. (b) Schematic of the surface treatment used for the MTJ biosensor array. (c) Optical image of the 64-element MTJ biosensor device. (d) A close-up view of the active arms of the array, each of which contains 16 MTJ sensors.

sensitivity is minimized. An ac (100 Hz) magnetic field of 15 Oe (rms) is applied in the sensing direction to excite the magnetic NPs. The sensor is operated in an ac bridge configuration and the signal extracted using a lock-in technique. An Evolution™ LC charge coupled device camera was used to monitor the sensor surface, and also to capture real-time video and pictures.

The MTJ sensor surface was biologically treated, so as to be able to capture the functionalized NPs. The detailed surface treatment steps were described in a previous work.[11] Figure 1(b) shows an illustration of the sensor surface after this treatment has been completed. Fe_3O_4 NPs synthesized by our collaborators (16 nm in diameter; M_s=480 emu/cm^3) were used throughout this experiment.[15] These NPs are superparamagnetic and are surface coated with streptavidin groups. In order to quantitatively evaluate the sensor response in the presence of NPs, the relationship between the NPs coverage and the concentration of the target DNA needed to be determined. To do this, we first immobilized 40 μM probe DNA onto the sensor surface, then hybridized it with complementary target DNA at different concentrations, through the standard DNA hybridization process. The surfaces of all the samples were then examined by scanning electron microscopy after the bonding of Fe_3O_4 NPs with target DNAs. The IMAGE-PRO PLUS® image analysis software was used to count the NPs and calculate the total amount of coverage. Figure 2(a) plots the measured NPs coverage as a function of the target DNA concentration. This figure shows that the coverage of Fe_3O_4 NPs is proportional to the logarithm of the concentration of target DNA, which is consistent with results reported by other groups.[3] Notice that a significantly nonspecific bonding coverage (1.9%) was observed for our Fe_3O_4 NPs; this could be due to the existence of unwanted adhesion between the Fe_3O_4 particles and the polyethylenimine (PEI) layer.[7]

The real-time detection of target DNA molecules was carried out using a single 64-element MTJ bridge array. The sensor array surface was first immobilized with 40 μM probe DNA, followed by hybridization with a 2.5 μM complementary target DNA. The sensor chip was then sealed within the microfluidic channel and mounted onto the chip carrier, which was plugged into the amplification PCB. The purpose of the microfluidic channels is to reliably deliver 16 nm Fe_3O_4 NPs in solution to the sensor area. The details of microfluidic channel fabrication are described in a previous work.[10,11] Figure 2(b) shows a 300 μm wide microfluidic channel sealed on a chip containing an MTJ bridge. The channel design also contains a compartment to allow physi-

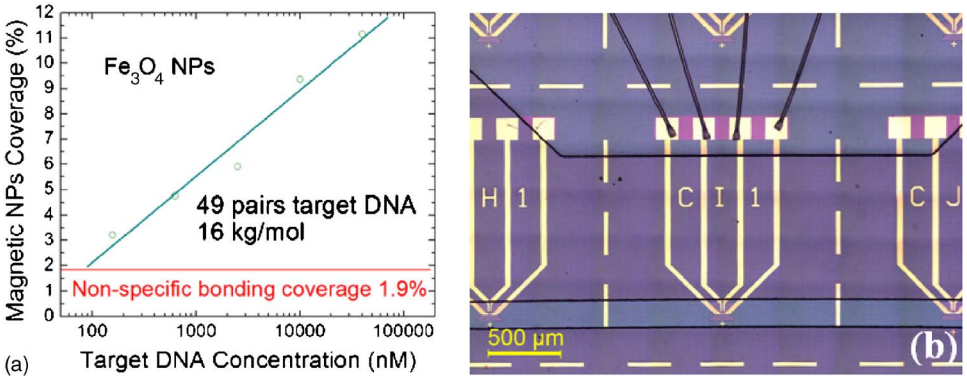

FIG. 2. (Color online) (a) Semilogarithmic graph plotting the coverage of Fe_3O_4 NPs vs the concentration of target DNA. (b) A 300 μm wide microfluidic channel sealed on the MTJ bridge array chip.

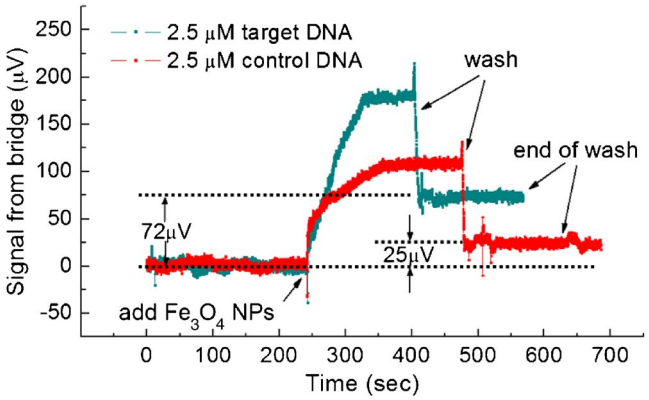

FIG. 3. (Color online) Real-time detection data of 2.5 μM target DNA (dark cyan curve) and 2.5 μM control DNA (red curve) by the MTJ biosensor.

cal access to the MTJ contact pads for wire bonding. The adhesion between the microfluidic structure and the biosensor chip is not permanent so that channels can be removed and/or reused for multiple sensor die.

Figure 3 plots the real-time detection data of Fe_3O_4 NPs for both complementary target DNA and noncomplementary control DNA. The microfluidic channel was first flushed with phosphate buffer solution (PBS) buffer to allow the system to stabilize for about 4 min. Fe_3O_4 NPs in a de-ionized water solution were then injected into the microfluidic channel by a syringe pump (World Precision Instruments' SP101i). After the NPs reached the sensor array, the syringe pump was stopped to allow the NP's settling onto the sensor array surface. At this point, the MTJ array's output signal increased monotonically until saturation was reached after about 1 min. The Fe_3O_4 NPs yielded a saturation signal of 180 μV_{rms} with an excellent signal-to-noise ratio. About 2 min after the signal stabilized, the sensor surface was again flushed with PBS buffer to remove nonspecifically bonded NPs. The residual signal of 72 μV_{rms} corresponds to the signal from the specifically bonded NPs remaining on the MTJ sensor array after the wash. This signal is directly attributable to the presence of the 2.5 μM complementary target DNA strands.

For comparison, we also measured real-time signals from Fe_3O_4 NPs with 2.5 μM of control DNA. The control DNA, which has biotin at the 3 ft end, is not complementary to the probe DNA anchored on the sensor surface. Therefore, ideally there should be no biotin end-labeled DNA strands left after the DNA hybridization process. However, due to the nonspecific bonding between control DNA and probe DNA strands, and/or unwanted bonding between NPs and the PEI polymer layer, some NPs can still bond to the sensor surface. This resulted in an unwanted residual signal (25 μV), the magnitude of which can be used to estimate the system detection limits. If we assume that the MTJ biosensor's output is proportional to the coverage of Fe_3O_4, i.e., to the logarithm of target DNA concentration from Fig. 2(a), we can estimate that our current system's detection limit of complementary target DNA is better than 100 nM. To further improve the system's detection limit, the specific bonding coverage of NPs can be increased, or alternatively the unspecific bonding rate of NPs can be reduced. If we assume that the unspecific bonding rate of NPs can be made negligible, the system's detection limit is then determined by the intrinsic noise of the MTJ sensors, which is about 7 μV, derived from the standard deviation of the flat parts of the bridge output voltage shown in Fig. 3. Translating this figure into a target DNA concentration using Fig. 2(a), we arrive at an effective detection limit of ~2 nM or ~33 pg/μl. These results are comparable to earlier results from the GMR-based bead array counter sensor,[16] and superior to conventional techniques using florescent markers.[3]

In summary, we have designed and developed MgO-based MTJ bridge arrays for the detection of DNA strands labeled with 16 nm Fe_3O_4 NPs. We demonstrated the detection of 2.5 μM single-strand DNA after the DNA hybridization process, obtaining a signal of 72 μV from complementary target DNA and a nonspecific bonding signal of 25 μV from noncomplementary control DNA. These values indicate that our current system's detection limit of analyte DNA is better than 100 nM, which is very promising for the high-sensitivity detection of DNA and/or proteins in the future.

At Brown, this work was supported by the National Science Foundation Grant No. DMR-0605966 and by JHU MRSEC (NSF DMR-0520491). At Micro Magnetics, this work was supported by the National Science Foundation Grant No. DMR-0611054. The authors wish to thank J. Xie, C. Xu, S. H. Sun, X. Y. Liu, and D. Mazumdar for discussion and assistance.

[1] G. Reiss, H. Brueckl, A. Huetten, J. Schotter, M. Brzeska, M. Panhorst, D. Sudfeld, A. Becker, P. B. Kamp, A. Puehler, K. Wojczykowski, and P. Jutzi, J. Mater. Res. **20**, 3294 (2005).
[2] D. L. Graham, H. A. Ferreira, and P. P. Freitas, Trends Biotechnol. **22**, 455 (2004).
[3] J. Schotter, P. B. Kamp, A. Becker, A. Puhler, G. Reiss, and H. Bruckl, Biosens. Bioelectron. **19**, 1149 (2004).
[4] M. Megens and M. Prins, J. Magn. Magn. Mater. **293**, 702 (2005).
[5] M. Piedade, L. A. Sousa, T. M. de Almeida, J. Germano, B. D. da Costa, J. M. Lemos, P. P. Freitas, H. A. Ferreira, and F. A. Cardoso, IEEE Trans. Circuits Syst., I: Regul. Pap. **53**, 2384 (2006).
[6] Q. A. Pankhurst, J. Connolly, S. K. Jones, and J. Dobson, J. Phys. D: Appl. Phys. **36**, R167 (2003).
[7] G. X. Li, S. H. Sun, R. J. Wilson, R. L. White, N. Pourmand, and S. X. Wang, Sens. Actuators, A **126**, 98 (2006).
[8] I. Zutic, J. Fabian, and S. Das Sarma, Rev. Mod. Phys. **76**, 323 (2004).
[9] S. X. Wang, S. Y. Bae, G. X. Li, S. H. Sun, R. L. White, J. T. Kemp, and C. D. Webb, J. Magn. Magn. Mater. **293**, 731 (2005).
[10] W. F. Shen, X. Y. Liu, D. Mazumdar, and G. Xiao, Appl. Phys. Lett. **86**, 253901 (2005).
[11] W. F. Shen, B. D. Schrag, M. J. Carter, J. Xie, C. J. Xu, S. H. Sun, and G. Xiao, J. Appl. Phys. **103**, 07A306 (2008).
[12] S. S. P. Parkin, C. Kaiser, A. Panchula, P. M. Rice, B. Hughes, M. Samant, and S. H. Yang, Nat. Mater. **3**, 862 (2004).
[13] S. Yuasa, T. Nagahama, A. Fukushima, Y. Suzuki, and K. Ando, Nat. Mater. **3**, 868 (2004).
[14] W. F. Shen, D. Mazumdar, X. J. Zou, X. Y. Liu, B. D. Schrag, and G. Xiao, Appl. Phys. Lett. **88**, 182508 (2006).
[15] S. H. Sun, Adv. Mater. (Weinheim, Ger.) **18**, 393 (2006).
[16] R. L. Edelstein, C. R. Tamanaha, P. E. Sheehan, M. M. Miller, D. R. Baselt, L. J. Whitman, and R. J. Colton, Biosens. Bioelectron. **14**, 805 (2000).